ELSEVIER

Journal of Crystal Growth 166 (1996) 669–674

JOURNAL OF CRYSTAL GROWTH

Influence of crucible and crystal rotation on oxygen-concentration distribution in large-diameter silicon single crystals

Isao Kanda [a,*], Takefumi Suzuki [b], Kiyoshi Kojima [c]

[a] Electronics Research Laboratories, Nippon Steel Corporation, 3434 Shimata Hikari Yamaguchi Pref. 743, Japan
[b] Process Technology Research Laboratories, 20-1 Shintomi Futtsu Chiba Pref. 299-12, Japan
[c] Manufacturing Department, NSC Electron Corporation, 3434 Shimata Hikari Yamaguchi Pref. 743, Japan

Abstract

The influence of crystal and crucible rotation rate on the oxygen-concentration distribution in 8 inch crystals grown from 18 inch crucibles is investigated both by growth experiments and by water-model melt-flow simulation. Differing from previous studies, the following behaviour is obtained: (1) After the shoulder transition region, increasing seed rotation (S/R) decreases oxygen concentration: this effect is enhanced by lowering the crucible rotation (C/R). (2) Under S/R > 9 rpm, radial variation of the oxygen concentration increases as C/R increases (15 > 10 > 5 rpm), but under S/R < 9 rpm, this order changes to C/R = 10 > 15 > 5 rpm. With careful consideration for the balance between natural and forced convection, internal motion of the silicon melt is simulated by a water-model method. In the axial section, stable radially outward flow is observed below the free surface. The sweep length of this flow on the free surface increases as the ratio of the Reynolds number of crystal rotation to that of crucible rotation increases. By combining the near-surface flow pattern and evaporation of SiO, a model is proposed that describes well the oxygen concentration behaviours.

1. Introduction

Interstitial oxygen is the main impurity in silicon single crystals grown by the conventional Czochralski method. Oxygen plays both beneficial and detrimental roles in electronic device manufacturing: oxygen precipitates *beneath* the active device region act as gettering sites for metallic impurities, while those *in* the active device region cause junction breakdown or leakage current. Therefore, a proper range of oxygen concentration does exist for each device process, and many researchers have investigated oxygen-control techniques in the crystal-growth process.

In the oxygen transportation mechanism, oxygen enters into the silicon melt from a silica crucible [1,2]. The dissolution rate of the crucible by the melt depends on temperature, adjacent melt flow rate, and surface condition of the crucible, along with other factors [1,3]. It is transported by diffusion, natural convection, and forced convection driven by crucible and crystal rotation. Most of the oxygen then reaches the free surface and evaporates as SiO. The rest is incorporated in the growing crystal according to a segregation mechanism.

To control oxygen concentration, changing crucible and crystal rotation rates is commonly used, resulting in the following: (1) Oxygen concentration increases as the crucible rotation rate (C/R) increases [1,2]. (2) Oxygen concentration increases as

* Corresponding author.

SSDI 0022-0248(95)00494-7

the crystal rotation rate, or "seed rotation rate" (S/R), increases if no force, such as a horizontal magnetic field, suppresses vertical motion of the melt [1,4–6]. (3) As the S/R increases, radial distribution of oxygen concentration becomes flatter [2]; this effect is suppressed by increasing C/R [7].

Because of the growing demand for larger-diameter silicon wafers, crystal growth systems have become larger. As a consequence, the above knowledge, obtained with various sizes of crystals and crucibles by which the melt flow is influenced, is not always applicable to the current manufacturing system. In this paper, we present another example of oxygen-concentration behaviour in a commercial-size system and relate it to the convection of the silicon melt.

First, we measured the oxygen-concentration distribution of silicon single crystals grown under various S/R and C/R. Then, with careful consideration for the balance between natural and forced convection, we examined the internal motion of the silicon melt by a model Czochralski melt that employs water as a working fluid.

2. Crystal growth

2.1. Experimental procedure

Three silicon single crystals of 8 inch diameter were grown from 18 inch diameter silica crucibles (see Table 1). The crystals and crucibles were rotated in opposite directions. In each crystal growth, S/R was (1) decreased in proportion to the body length from 16 rpm at the shoulder to 5 rpm at the body length of 160 mm and (2) increased linearly back to 16 rpm at the body length of 320 mm. C/R was set at 5, 10 and 15 rpm respectively.

Table 1
Growth apparatus and growth conditions

Furnace	DP-3800RW (KOKUSAI ELECTRIC)
Charge of polycrystalline silicon	50 kg (Melt depth 164 mm)
Crucible	Mitsubishi material quartz CR20
Crucible inner radius	222 mm
Ambient	Purified argon Volume flow rate 0.1 m^3/min
Crystal radius	105 mm
Crystal orientation	⟨100⟩
Dopant	Boron
Seed lift rate	Between 0.6 and 0.8 mm/min

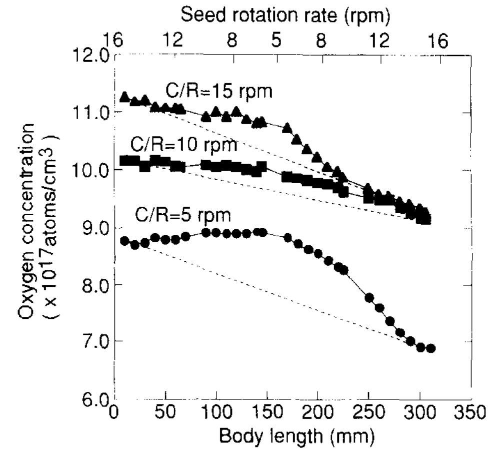

Fig. 1. Axial distribution of the oxygen concentration at the center of the crystals. In the first half of the body, the oxygen concentration decrease is suppressed as seed rotation rate decreases.

Each crystal was divided equally into four blocks and sliced along the growth axis into 1 mm thick samples. Both surfaces of the samples were lapped, and then one side was polished. Using the JEIDA standard conversion coefficient, the oxygen concentration was measured by FT-IR (BIO-RAD DIGILAB FTS-40). The measurement spacing was 10 mm in both axial and radial directions. The standard deviation of the measurement was 0.04×10^{17} atoms/cm^3.

2.2. Results

The axial distribution of the oxygen concentration is shown in Fig. 1. Oxygen concentration is high under high C/R because of the high crucible wall temperature, and it decreases with the body length because the contact area of the silicon melt with the crucible decreases. Note that, in the first half of the body, as S/R decreases, the decrease of oxygen concentration is suppressed, and the suppression effect is enhanced under a lower C/R. For the crystal with C/R = 5 rpm, the concentration actually increases. Increasing S/R was previously known to increase oxygen concentration, which is attributed to

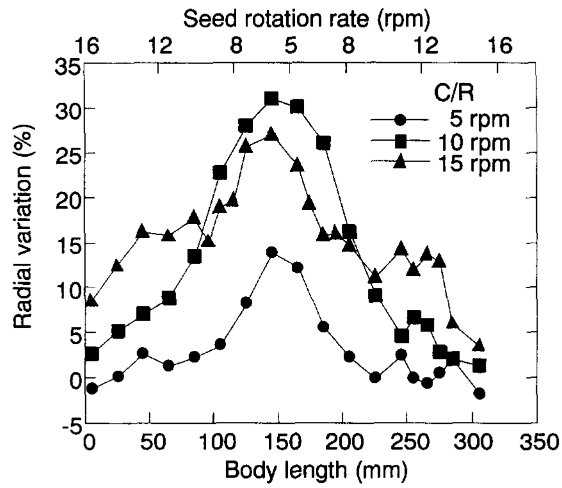

Fig. 2. Radial variation of oxygen concentration as a function of S/R and C/R.

the "pumping flow" from the oxygen-rich crucible bottom region to the solidifying interface [1,4–6]. Under the experimental condition here, however, the "pumping flow" likely did not reach the crucible bottom (the melt depth was 120 mm at crystal body length of 160 mm). Thus, some other S/R-related factors must decrease oxygen concentration at high S/R.

The axial distribution of the radial variation of oxygen concentration is shown in Fig. 2. The radial variation of oxygen concentration is defined as:

$$\text{Radial variation}\ (\%) = (A - B)/B \times 100, \qquad (1)$$

where A and B are the oxygen concentration at the center and 15 mm from edge respectively. Like previous studies [2], under higher S/R, the radial variation decreases. Note that, under S/R > 9 rpm, the radial variation increases as C/R increases (15 $> 10 > 5$ rpm), but under S/R < 9 rpm, this order changes to $10 > 15 > 5$ rpm. In Ref. [7] the authors point out that increasing C/R suppresses the effect of crystal rotation, but here it is found to be more complex.

3. Water model

3.1. Physical meaning

The internal motion of a silicon melt has been studied using various methods. Numerical simulation is expected to give conclusive information, but because the lack of reliable knowledge of physical constants lessens its reliability, research is still being conducted to determine these constants [8]. Recently, direct observation by X-ray was carried out [9] to visualize the streak line of the melt, but it was difficult to examine the macroscopic stream lines because the melt flow is time-dependent. The water-model method can be easily used to visualize the internal motion of the melt and has been applied to Czochralski melts of oxides [10], the Prandtl number of which is near that of water. Although the Prandtl number of silicon is two orders of magnitude smaller than that of water and although the water-model method is regarded as not suitable for silicon melt, valuable information can still be obtained if the conditions are carefully selected. Therefore, we employed the water-model method and focused on the interaction of the forced convection driven by crucible and crystal rotations because the kinematic viscosity of the silicon melt and water are on the same order. We selected the model conditions so that Gr/Re_c is similar to a silicon melt because the melt convection is a mixture of forced and natural convection [9,11]. Here Gr and Re_c are the Grashof and Reynolds numbers of crucible rotation defined as:

$$Gr = g\beta(\Delta T)d^3/\nu^2, \qquad (2)$$

$$Re_c = R_c^2\omega_c/\nu, \qquad (3)$$

where g, β, ΔT, d, ν, R_c and ω_c are the acceleration of gravity, the volume expansion coefficient, the vertical temperature difference, the depth of the fluid, the kinematic viscosity, the crucible radius, and the angular velocity of the crucible respectively. The values of these constants are listed in Table 2.

3.2. Apparatus

The water-model apparatus is shown schematically in Fig. 3. The size was about half of the CZ furnace used in the crystal-growth experiment, except the crystal radius was 1.5 inch, which was based on 6 inch real crystals. Made of acrylic resin, the "crucible" had a shape similar to that of the actual silica crucible. The "crystal" was a flat-bottomed stainless steel cylinder with the bottom surface cooled by ice. The "crucible" was surrounded by hot water jackets with separations to give a vertical tempera-

Table 2
Values of volume expansion coefficient, β, vertical temperature difference, ΔT, kinematic viscosity, ν, depth of fluid, d, crucible radius, R_c, angular velocity of the crucible, ω_c, Grashof number, Gr, Reynolds number of crucible rotation, Re_c, and the ratio Gr/Re_c; ΔT of the silicon melt is an estimated value; d of the silicon melt is the depth at the crystal shoulder

	β (deg^{-1})	ΔT (deg)	ν ($m^2 s^{-1}$)	d (m)	R_c (m)	ω_c (rpm)	ω_c (rad s^{-1})	Gr	Re_c	Gr/Re_c
						2	2.09×10^{-1}		2.12×10^3	1.55×10^4
Water (300 K)	0.26×10^{-3}	20	8.91×10^{-7}	8.0×10^{-2}	9.50×10^{-2}			3.29×10^7		
						18	1.88		1.91×10^4	1.72×10^3
						5	5.24×10^{-1}		8.31×10^4	2.35×10^4
Silicon (1700 K)	1.50×10^{-3}	40	3.20×10^{-7}	1.5×10^{-1}	2.25×10^{-1}			1.95×10^9		
						15	1.57		2.49×10^5	0.78×10^4

ture difference. Both the "crucible" and "crystal" rotate around the axis. The working fluid was water with thermochromic liquid capsules (diameter: 10–20 μm, density: 1.01–1.02 g/cm^3). To observe the fluid motion in the axial section, light from a xenon lamp was radiated in a plane along the axis in a dark room, and the thermochromic liquid capsules were seen in colors representing the corresponding temperatures.

The depth of the fluid was 80 mm. The "crystal" and "crucible" were rotated in opposite directions with S/R ranging from 0 to 54 rpm and C/R from 0 to 18 rpm. The temperature difference was not intentionally set between the upper and lower hot water jacket. The temperature of the inner surface of the "crucible" fluctuated between 20 and 25°C, which was measured by a thermocouple. The temperature difference between the crucible wall and the crystal drives the natural convection.

3.3. Observations

Just below the free surface, stable radially outward flow was observed (Fig. 4). The flow in other region was unstable, and it was difficult to determine the stream line; therefore, no upward flow from the crucible bottom to the growing interface was observed. The radially outward flow had the following

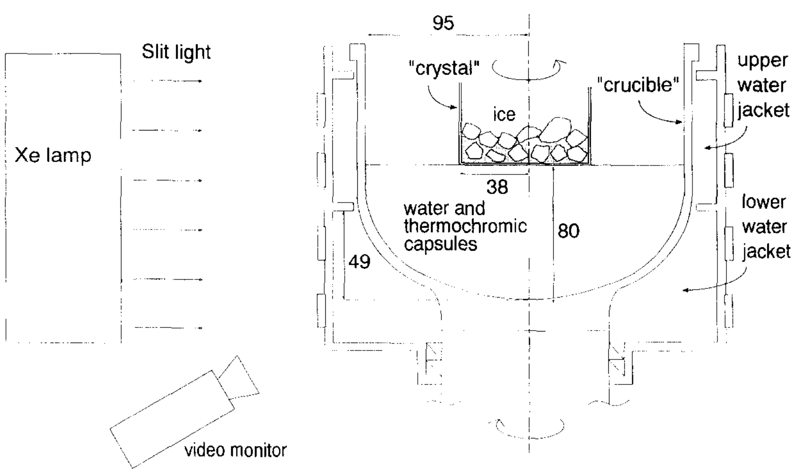

Fig. 3. Axial-section view of the water-model apparatus. "Crucible" and water jackets are made of acrylic resin. The fluid motion in this section is visualized by the light from a xenon lamp. The unit of length is millimeters.

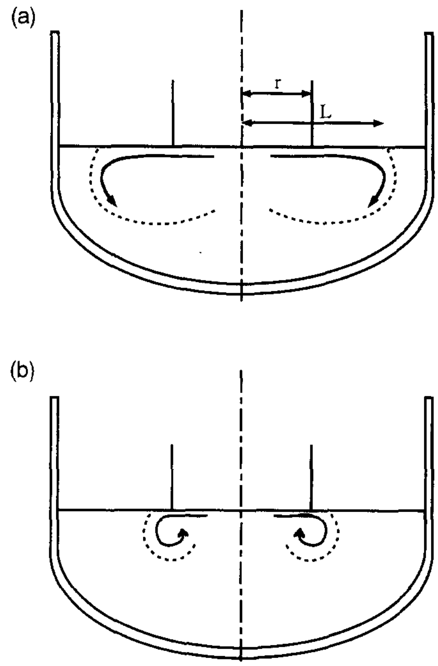

Fig. 4. Characteristic flow patterns observed in the water-model experiment. Arrows represent the vertical plane component of stream lines. Inside the dotted lines are regions, in case of silicon melt, where the oxygen concentration is lowered by SiO evaporation and mostly effects the concentration in silicon crystals. (a) High S/R and low C/R (large Re_s/Re_c); (b) low S/R and high C/R (small Re_s/Re_c).

characteristics depending on the combination of C/R and S/R: Under low C/R and high S/R [Fig. 4a], the fluid was swept far from the crystal edge where it sank and was mixed with the bulk flow. Under high C/R and low S/R [Fig. 4b], it was swept a short distance where it sank, was pumped up, and was again swept from the crystal edge. Under S/R = 0 rpm and C/R = 0 rpm, only natural convection existed, and below the free surface, radially inward flow, which sank at the axis, was observed. The normalized sweep length $(L-r)/r$ is shown versus Re_s/Re_c in Fig. 5, where L, r and Re_s are the distance between the axis and the "sinking point", the "crystal" radius, and the Reynolds number of crystal rotation respectively. Re_s is defined as:

$$Re_s = r^2\omega_s/\nu, \tag{4}$$

where ω_s is S/R.

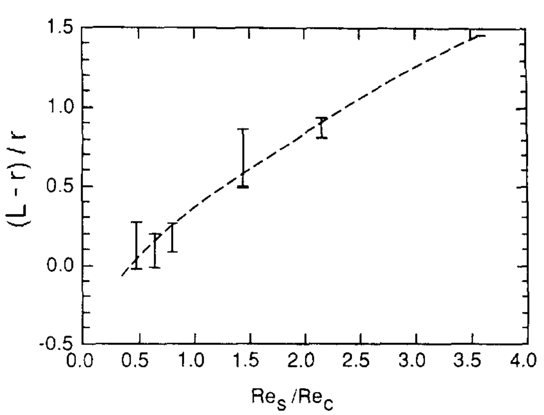

Fig. 5. Normalized sweep length of radially outward flow.

4. Discussion

Because the segregation coefficient of oxygen is not well determined [4,12], we attempted to explain the oxygen concentration distribution behaviour by melt convection and SiO evaporation. The evaporation depends on the flow condition near the gas–liquid interface. Because the gas flow condition was not changed in this experiment, the surface flow of the melt has the main effect on SiO evaporation. The surface flow can be classified into four categories. In order of dominance, the first is the rotating flow around the axis with almost the same angular velocity as the crucible, the second is the above-mentioned radially outward flow from the crystal edge, the third is the eddies in the surface plane caused by baroclinic instability [11], and fourth is the surface-tension flow toward the edge of the crystal [2]. Among these, the second flow has a relatively large velocity and sweeps a wide area caused by crystal rotation. We propose a model to associate this radially outward flow with SiO evaporation and to explain the distribution of oxygen concentration.

We assume that the evaporation rate of SiO from a fluid element is constant along this radially outward flow. Such a fluid element is projected from the crystal edge with an average radial velocity component v and sinks into the bulk melt a distance $L-r$ away from the crystal edge. The amount of SiO that evaporates from this one element is proportional to $(L-r)/v$. Because the number of fluid elements projected from the crystal edge in a unit time is thus proportional to v, the amount of oxygen that evaporates from this radially outward flow region in a unit time is thus in proportion to $L - r$.

Under low S/R and high C/R (small Re_s/Re_c), $L - r$ is small and the flow circulates near the crystal edge, as observed in the water-model experiment. This implies that only a little oxygen evaporates and that a localized low-oxygen region is formed near the crystal edge. On the other hand, under high S/R and low C/R (large Re_s/Re_c), $L - r$ is large and the flow is mixed with the bulk melt, implying that the amount of evaporating oxygen is large and that a relatively uniform low-oxygen region is formed under the growing interface.

This model assumes that the radially outward flow goes over the crystal edge, and it explains well the observed oxygen-concentration behaviour as follows: (1) Lowering S/R reduces the amount of oxygen evaporated from the bulk of the silicon melt to suppress the decrease of oxygen concentration, and the effect is enhanced under lower C/R because the change in Re_s/Re_c is larger for the same change in S/R. (2) The radial variation of oxygen concentration is larger under lower S/R and higher C/R, but this model does not explain the radial variation under S/R < 9 rpm and C/R = 15 rpm ($Re_s/Re_c < 0.13$). The radially outward flow probably does not go over the crystal edge under such low Re_s/Re_c conditions. The critical values of S/R and C/R for $L < r$ cannot be determined by the water-model experiment because the silicon melt and water are quite different fluids.

5. Summary

In this study, the following behaviour was found to be different from previous studies: (1) Decreasing S/R increases the oxygen concentration, and the effect is enhanced by lowering C/R. (2) Under S/R > 9 rpm, radial variation increases as C/R increases (15 > 10 > 5 rpm), but under S/R < 9 rpm, this order changes to C/R = 10 > 15 > 5 rpm.

To simulate the internal motion of the silicon melt, water-model method is employed. In the axial section, stable radially outward flow is observed just below the free surface. Its sweep length on the surface increases as Re_s/Re_c increases. In view of convection and evaporation, the oxygen concentration behaviour can be explained by the SiO evaporation from this radially outward flow.

Acknowledgements

The authors thank S. Shinoyama, H. Haga, H. Harada, M. Hasebe, S. Takao, M. Tanaka and T. Yamauchi for reviewing the paper and discussion.

References

[1] J. W. Moody, Semicond. Silicon 1986 (1986) 100.
[2] W. Zulehner, Semicond. Silicon 1989 (1989) 2.
[3] H. Hirata and K. Hoshikawa, Jpn. J. Appl. Phys. 19 (1980) 1573.
[4] C.T. Yen and W.A. Tiller, J. Crystal Growth 109 (1991) 142.
[5] M. Ohwa et al., Semicond Silicon 1986 (1986) 117.
[6] K.G. Barraclough, R.W. Series, G.J. Rae and D.S. Kemp, Semicond. Silicon 1986 (1986) 129.
[7] J. Leroueille and P. Philippot, IBM Tech. Disclosure Bull. 27 (1985) 4817.
[8] H. Sasaki, E. Tokizaki, K. Terashima and S. Kimura, Jpn. J. Appl. Phys. 33 (1994) 3803.
[9] K. Kakimoto, M. Eguchi, H. Watanabe and T. Hibiya, J. Crystal Growth 88 (1988) 365.
[10] A. D. W. Jones, J. Crystal Growth 94 (1989) 421.
[11] Y. Kishida, M. Tanaka and H. Esaka, J. Crystal Growth 130 (1993) 75.
[12] E. Iino, I. Fusegawa and H. Yamagishi, Mater. Sci. Forum 117–118 (1993) 189.